

*Article*

## Synthesis and Characterization of Bimodal Mesoporous Silica Derived from Rice Husk Ash

Chanyarak Watthanachai<sup>1,a</sup>, Chawalit Ngamcharussrivichai<sup>2</sup>, and Somchai Pengprecha<sup>3,b,\*</sup>

<sup>1</sup> Interdisciplinary Program in Environmental Science, Graduate School, Chulalongkorn University, Bangkok 10330, Thailand

<sup>2</sup> Center of Excellence on Catalysis for Bioenergy and Renewable Chemicals (CBRC), Faculty of Science, Chulalongkorn University, Bangkok 10330, Thailand

<sup>3</sup> Department of Chemistry, Faculty of Science, Chulalongkorn University, Bangkok 10330, Thailand  
E-mail: <sup>a</sup>chanyarak360fox@gmail.com, <sup>b</sup>spengprecha@hotmail.com (Corresponding author)

**Abstract.** This study was able to obtain bimodal mesoporous silica through a process of synthesizing silica derived from rice husk ash in conjunction with structure-directing agents (Pluronic P123 and cetyltrimethyl ammonium bromide (CTAB)) and the application of the sol-gel method. Rice husk ash taken from a biomass power plant went through a process of extraction using sodium hydroxide. The procedures of X-ray diffraction, X-ray fluorescence spectrometer, Fourier-transform infrared spectrometer, N<sub>2</sub> adsorption-desorption isotherm, Transmission electron microscope and Scanning electron microscope techniques in order to perform the characteristics of bimodal mesoporous silica (BMS), unimodal mesoporous silica with Pluronic P123 (UMS-P123), unimodal mesoporous silica with cetyltrimethyl ammonium bromide (UMS-CTAB) and rice husk silica (RHS). The results showed that bimodal mesoporous silica with the prominent characteristic of larger mesopore were created when materials such as SBA-15 (the dominant characteristics of Pluronic P123), and with CTAB incorporated, in which the mesopore in a smaller size originated from parent templates. The specific surface area ( $>700$  m<sup>2</sup>/g), pore volume (1.30 cm<sup>3</sup>/g) and pore size (9.20 and 3.30 nm) of bimodal mesoporous silica was found to be higher unimodal mesoporous silica (UMS-P123 and UMS-CTAB). Consequently, bimodal mesoporous silica synthesize from rice husk ash is considered to be a very suitable material which has the potential to be applied for an adsorbent and also gave the environment benefits and renewable resource.

**Keywords:** Bimodal mesoporous silica (BMS), unimodal mesoporous silica (UMS), rice husk silica (RHS), rice husk ash, sol-gel.

ENGINEERING JOURNAL Volume 23 Issue 1

Received 8 June 2018

Accepted 11 November 2018

Published 31 January 2019

Online at <http://www.engj.org/>

DOI:10.4186/ej.2019.23.1.25

## 1. Introduction

There is a lot of interest in materials identified as being 'bimodal mesoporous (BM)' due to the fact that it can be used as an absorbent and a catalyst. However, bimodal mesoporous materials require a specific size (particularly in terms of pores) while the structure also has to be specific in order to be able to be assigned to the self-assembly of the structure-directing templates or agents. There are two different types of pore structures found on varying sizes of bimodal mesoporous materials and these ranging from 2 - 50 nm. In order to propose the range of area for an adsorption/catalytic reaction, small pores are applied while in the promotion of diffusion at the molecule level, large pores are applied [1]. Consequently, the surface of BM materials is high which helps the wide-scale transportation in hierarchical structure of pores. To synthesize the BM, various types of techniques can be used, such as catalytic [2] bioengineering [3] and adsorption [4, 5]. Nowadays, the bimodal mesoporous materials are well known as a bimodal mesoporous silica (or BMS). These are applied in the indication process of synthesis. It should also be noted that the pore structure design includes a framework where the distribution and surface size of the pores can be controlled [6]. The synthesis of BMS can use differing types of process, namely flame-spray pyrolysis, sol-gel process and precipitation method [7]. However, the sol-gel process is deemed to be most effective for BMS synthesis because this method is relatively straightforward and simple to carry out. Recently, Zhang et al. [8] (in a follow up to the sol-gel process) used mixed templates of liquid paraffin as a swelling agent together with triblock copolymer P123 in the water/oil (W/O) surface for the synthesis of BMS. The material used in the study was reported to have small pores in the range of 5 - 10 nm and large pores of 30 nm. Renewable resources can be used to synthesize these BM materials, for example, rice husk ash (silica source) may be used together with chitosan for the template for the synthesis of bimodal porous silica [9]. Jullaphan et al. [10] also synthesized bimodal mesoporous silica (BMS) by sol-gel process with using rice husk ash and Pluronic P123 and cetyltrimethyl ammonium bromide (CTAB) as the structure-directing agents (mixing phases of the large pore of SBA-15 and the small pore of SBA-3-like in silica). In addition, BMS was prepared with CTAB templates for small mesopores (MCM-41) and silica gel for large mesopores that were applied as part of the sol-gel process [11]. Recently, Yang et al. [1] also revealed the developed synthesis of BMS materials with two coexisting phases (hexagonal and semi-cubic) by a co-hydrothermal aging route with the gel containing P123 and F127.

Typically, silica is used as an inorganic precursor for the synthesis of BMS materials. Sodium silicate and tetraethyl orthosilicate (TEOS) are generally the most readily-available sources of silica [2, 7, 12]. The characteristics of the surfactants have to be selected (size of the pores, surface area and type of structure). As an example, a cationic surfactant of CTAB and nonionic surfactant of a triblock-copolymer [13]. It has been reported that different variable factors can have an effect these processes, for example, synthetic temperature and media can have an effect on mesostructures and also hydrothermal treatment associates with growth and crystallization during the synthesis [6]. Therefore, there is a need to find renewable sources in order to reduce the raw materials costs, and to give environment benefits. Rice husk ash or RHA is the one material contained a significant quantity of silica [14-17], especially, RHA was collected as the waste product from a biomass power plant in Thailand's Phichit, a province in the north-central region of the country. The best way to prepare rice husk ash is to employ a base extraction method [16-20], whereby the obtained material can be used as a raw material to generate inorganic precursor or sodium silicate.

Consequently, this research employed a method of sol-gel process with the aim of using a mix of sodium silicate (from RHA) with Pluronic P123 and CTAB (or structure-directing agents) to synthesize BMS (bimodal mesoporous silica). Procedures of XRD, XRF, FT-IR, N<sub>2</sub> adsorption-desorption isotherm, TEM and SEM techniques were employed in order to characterize the physical and mesostructured properties of the samples. This study provides an important approach to synthesize ordered bimodal mesoporous silica that could find the applications in adsorbent.

## 2. Experimental Procedure

### 2.1. Material and Chemical Reagents

Rice husk ash (RHA) was obtained from biomass power plant in Phichit province, Thailand. The pore structure-directing agents (Pluronic P123 (EO<sub>20</sub>PO<sub>70</sub>EO<sub>20</sub>/PEO-PPO-PEO) and cetyltrimethyl ammonium bromide (CTAB or C<sub>16</sub>H<sub>33</sub>N (CH<sub>3</sub>)<sub>3</sub>Br) were purchased from Fluka and Sigma-Aldrich, respectively. All chemicals including NaOH, H<sub>2</sub>SO<sub>4</sub>, NH<sub>4</sub>OH and HCl used in the experiments were analytical grade.

## 2.2. Preparation of Sodium Silicate (SS)

To a 500 mL round bottom flask was charged with gray rice husk ash (10.00 g) in NaOH solution (80.0 mL, 2.50 N). The mixture was heated to 100°C with stirring and maintained for 3 h [20] before being filtered through a Whatman (No.1) filter paper, and the residual was washed with 20 mL of warm water. The filtrate was set to cool to room temperature. Finally, the sodium silicate (SS) was obtained and stored in a capped glass bottle for future use [15]. In order to prepare the rice husk silica (RHS), the pH of the filtrate or SS was adjusted with H<sub>2</sub>SO<sub>4</sub> solution (5.00 N) to a pH of 2 and adjusted back with NH<sub>4</sub>OH to a pH of 8.5. Subsequently, the mixture was allowed to stand for 3 h. Then, the mixture was filtered (Whatman No.1), and the residual was washed with warm water until the pH was 7 before being dried at 105°C for 12 h. Finally, RHS was ground and screened through 100 - 120 mesh size sieve (0.125 - 0.149 mm) and stored in a capped glass bottle for future use.

## 2.3. Synthesis of Bimodal Mesoporous Silica (BMS)

Bimodal mesoporous silica (BMS) was prepared from sodium silicate with the structure-directing agents using sol-gel technique. The synthesis of BMS was based on the molar ratio of 1SiO<sub>2</sub>: 0.0875Pluronic P123: 0.0875CTAB: 4HCl: 200H<sub>2</sub>O [10]. In 250-mL beaker, the solution of charged with Pluronic P123 (1.70 g, 0.0875 M) in HCl solution (50.0 mL, 2.00 M) was heated to 40°C with stirring until the homogenous solution. Then sodium silicate (11.0 mL, 1.00 M) was added and maintained at 40°C for 24 h. In the reaction mixture, the solution of CTAB (1.70 g, 0.0875 M) in HCl solution (50.0 mL, 2.00 M) was added and stirred at 40°C for 15 min. After that, the reaction mixture was placed in an autoclave lined with Teflon and cured under hydrothermal condition at 100°C for 24 h. The white product was collected by filtration, washed with distilled water, dried at 140°C for 3 h and calcined at 600°C for 5 h. Finally, BMS was ground and screened through 100 – 120 mesh size sieve (0.125 - 0.149 mm) and stored in a capped glass bottle for future use.

## 2.4. Synthesis of Mesoporous Silica (UMS-P123 and UMS-CTAB)

UMS-P123 and UMS-CTAB are the two unimodal mesoporous silica types that prepared from sodium silicate (section 2.2). The synthesis of UMS-P123 is described as follows; in 250-mL beaker, the solution of charged with Pluronic P123 (1.70 g, 0.0875 M) in HCl solution (50.0 mL, 2.00 M) was heated at 40°C with stirring until the homogenous solution. Then adding the sodium silicate (11.0 mL, 1.00 M) into this solution was maintained at 40°C for 24 h [6]. After that, the mixture was placed in an autoclave lined with Teflon and cured under hydrothermal condition at 100°C for 24 h. The product was filtered, washed with distilled water, dried at 140°C for 3 h and calcined at 600°C for 5 h. Finally, UMS-P123 was ground and screened through 100 – 120 mesh size sieve. UMS-CTAB was prepared by sodium silicate, following the procedure described above UMS-P123 synthesis, using CTAB (1.70 g, 0.0875 M) instead of Pluronic P123. Finally, UMS-CTAB was ground and screened through 100 – 120 mesh size sieve.

## 2.5. Characterization

To analyze the structure, each of the samples was characterized with X-ray diffraction (XRD) and were recorded in the  $2\theta$  range from 0.2° to 70° ( $2\theta$ ) at 40 kV and 30 mA with Cu-K $\alpha$  radiation, a Bruker D8 Advance diffractometer. The quantity of SiO<sub>2</sub> and impurities in the samples were determined by X-ray fluorescence spectrometer (XRF), Bruker model S8 Tiger and the morphology, surface texture and porosity of samples were analyzed with a JEOL JEM-2100 Transmission electron microscope (TEM) and a JEOL JSM-7610F Scanning electron microscope (SEM). The functional groups of samples were identified by a Nicolet Impact 410 Fourier-transform infrared spectrometer (FT-IR) in the range of 600 - 4,000 cm<sup>-1</sup>. The N<sub>2</sub> adsorption-desorption isotherms of the samples were measured using a BELSORP-mini, BEL at liquid nitrogen temperature. Samples were degassed at 150°C for 2 h under vacuum. The specific surface area of the samples was calculated from the Brunauer-Emmett-Teller (BET) equation by assuming the nitrogen molecule area to be 0.162 nm<sup>2</sup>. The total pore volumes were measured from the liquid volume of adsorbate adsorbed (N<sub>2</sub>) at a relative pressure of 0.99. Moreover, the pore size distribution was determined with the Barrett-Joyner-Halenda (BJH) method applied on the adsorption hysteresis loop assuming a model of hexagonally ordered pores.

### 3. Result and Discussion

#### 3.1. Structure of BMS, UMS-P123, UMS-CTAB and RHS Materials

The structure of BMS, UMS-P123, UMS-CTAB and RHS materials were analysed by XRD. As shown in Fig. 1(a), all materials exhibited the main broad peak was found for each of these materials at  $2\theta$  of  $22^\circ$ . This can be identified as the amorphous phase of silica [19, 20]. Similarly, as identified in Fig. 1(b), it can be seen that one main peak (100) at  $2\theta$  of  $1.0^\circ$  was evident for BMS, UMS-P123 and UMS-CTAB materials; this particular peak suggests that most characteristic of mesoporous silica material are shown by the arrangement of molecular sieve in the low angle XRD patterns ( $2\theta = 0.2^\circ - 7.0^\circ$ ) [6]. The peaks of  $2\theta$  of  $1.8^\circ$ (110) and  $2.0^\circ$ (200) suggest pores were structured in a hexagonal shape across a 2D channel, and this is applicable for such materials as SBA-15 [7, 10]. The small peak was altered to a higher angle (for UMS P123), may indicate a relationship with the small reduction of the diameter of the pore (for UMS-P123). Consequently, it can be deemed that silica derived from rice husk ash was able to obtain bimodal mesoporous silica by using Pluronic P123 and CTAB to structure the pores, it can be also deemed that the structure of bimodal mesoporous silica is similar to SBA-15 as a mesoporous material. This is a significant characteristic of Pluronic P123 and incorporated of CTAB with an acidic condition such as UMS-P123 is used for the synthesis process [10].

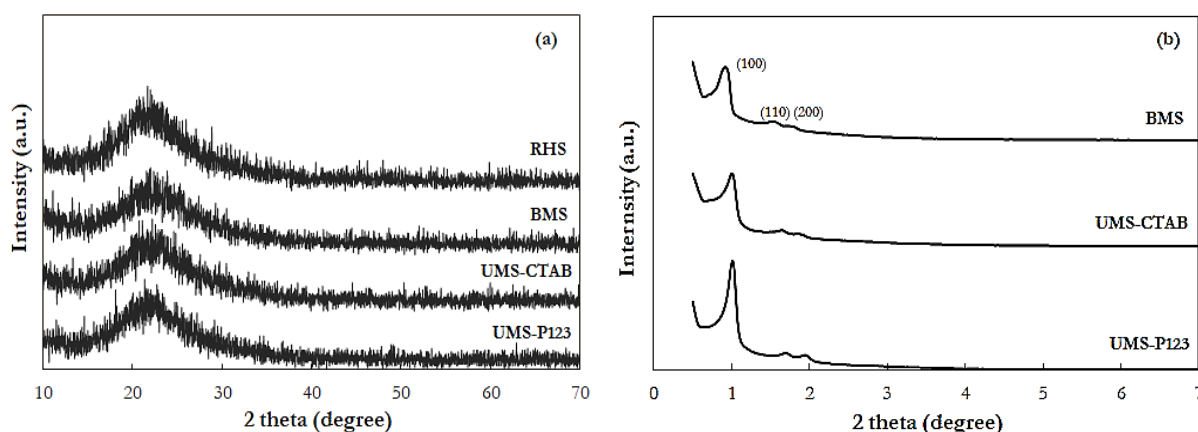


Fig. 1. XRD patterns of BMS, UMS-P123, UMS-CTAB and RHS materials.

#### 3.2. Elemental Composition

The elemental composition using X-ray fluorescence spectroscopy confirmed the high purity of RHS, BMS, UMS-P123 and UMS-CTAB materials are presented in Table 1.  $\text{SiO}_2$  amount of RHS, as compared to that of RHA, is 97.80 wt% due to it went through the extraction process, which silica dissolve well almost of other the composition be higher [18-20]. Also,  $\text{SiO}_2$  amount of BMS, UMS-P123 and UMS-CTAB materials are shown to be 99.97, 99.90 and 99.98 wt%, respectively. It can be concluded that BMS, UMS-P123 and UMS-CTAB materials are composed of  $\text{SiO}_2$ .

#### 3.3. Chemical Functional Groups

The FT-IR spectra of RHS, BMS, UMS-P123 and UMS-CTAB materials were recorded and are shown in Fig. 2 that confirmed the unimodal and bimodal mesoporous materials prepared from rice husk silica by using sol-gel technique. All materials in Fig. 2, the intense peaks at  $800$  and  $1,090$   $\text{cm}^{-1}$  may be attributed respectively to symmetric and asymmetric stretching vibration of the Si-O-Si bonds (siloxane group). It can be implied that all materials can be ascribed to composite of Si-O stretching in silica ( $\text{SiO}_2$ ) [15]. The spectra in the range of  $600 - 1,400$   $\text{cm}^{-1}$  are mostly the framework vibration characteristic of tetrahedron of silica with oxygen [13, 21, 22]. For RHS material, the broad peak at  $3,000 - 3,700$   $\text{cm}^{-1}$  and  $1,640$   $\text{cm}^{-1}$  are related to the stretching and bending vibration of the free hydroxyl groups or free water molecules [23, 24] and the Si-OH stretching of surface silanol hydrogen bond to molecular water, respectively [25]. A comparison of the

spectra of BMS, UMS-P123 and UMS-CTAB materials with the spectra of RHS showed the disappearance of peak position of 3,000 - 3,700 and 1,640  $\text{cm}^{-1}$  (hydroxyl stretching and bending vibration) due to stretching mode of broken Si-O bridges [22], that corresponds to the formation mode of Si-O-Si in bimodal mesoporous silica. It can be concluded that BMS, UMS-P123 and UMS-CTAB materials have been formed with  $\text{SiO}_2$  amorphous to form the bimodal mesoporous material [2, 11, 12], which is in accordance with the XRD results.

Table 1. Chemical composition of all materials as analyzed by X-ray fluorescence (XRF).

| Constituent as oxides (wt%) | RHA as raw material | RHS   | BMS   | UMS-P123 | UMS-CTAB |
|-----------------------------|---------------------|-------|-------|----------|----------|
| $\text{SiO}_2$              | 79.40               | 97.80 | 99.97 | 99.90    | 99.98    |
| $\text{K}_2\text{O}$        | 2.20                | 0.12  | <0.01 | <0.01    | <0.01    |
| $\text{CaO}$                | 0.80                | 1.06  | <0.01 | -        | -        |
| $\text{P}_2\text{O}_5$      | 0.73                | <0.01 | <0.01 | <0.01    | <0.01    |
| $\text{Al}_2\text{O}_3$     | 0.34                | 0.38  | -     | <0.01    | -        |
| Cl                          | 0.31                | 0.04  | <0.01 | 0.05     | <0.01    |
| $\text{MgO}$                | 0.30                | 0.29  | -     | -        | -        |
| $\text{Fe}_2\text{O}_3$     | 0.21                | 0.05  | 0.02  | 0.02     | 0.01     |
| $\text{MnO}$                | 0.16                | 0.03  | -     | -        | -        |
| $\text{SO}_3$               | 0.15                | <0.01 | <0.01 | <0.01    | <0.01    |
| $\text{CuO}$                | 0.02                | <0.01 | <0.01 | <0.01    | -        |
| $\text{ZnO}$                | 0.02                | 0.07  | <0.01 | -        | <0.01    |
| $\text{Na}_2\text{O}$       | <0.01               | 0.15  | -     | -        | <0.01    |
| Others                      | <0.01               | <0.01 | <0.01 | <0.01    | <0.01    |

Note: others ( $\text{CoO}$ , Br,  $\text{Y}_2\text{O}_3$ ,  $\text{ZrO}_2$ , I,  $\text{Dy}_2\text{O}_3$ ,  $\text{Er}_2\text{O}_3$ ,  $\text{SnO}_2$ ,  $\text{Cs}_2\text{O}$ ,  $\text{La}_2\text{O}_3$ ,  $\text{TiO}_2$ ,  $\text{Cr}_2\text{O}_3$ ,  $\text{Sc}_2\text{O}_3$ ,  $\text{Rb}_2\text{O}$ ).

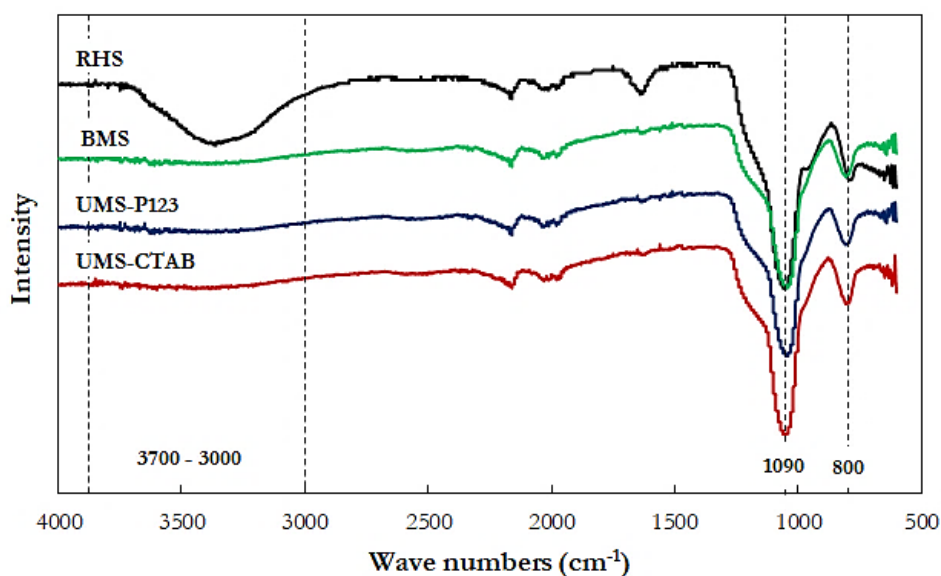


Fig. 2. FT-IR spectra of BMS, UMS-P123, UMS-CTAB and RHS materials.

### 3.4. Effect of Each Template/Structural Analysis

$\text{N}_2$  adsorption-desorption measurement is one of characteristic for analysis of mesoporous material that included the specific surface area, pore volume, pore size distribution and some properties of material. Figure 3 shows the  $\text{N}_2$  adsorption-desorption is the type IV isotherms in capillary condensation with H1 hysteresis loop according to IUPAC definition [6]. These indicated that the mesopore characteristic in cylindrical shape are existed. In the case of BMS, the type IV isotherm provided H1 hysteresis loop containing two capillary condensation at  $P/P_0$  of 0.30 - 0.70 and  $P > 0.70$  respectively, as seen in Fig. 3(a). That implied the bimodal

cylindrical mesopore shape are existed [6, 7, 26-28]. Meanwhile, the case of UMS-P123 and UMS-CTAB isotherms provided H1 hysteresis loop containing only one capillary condensation at  $P/P_0$  of 0.30 - 0.70 which implied the unimodal cylindrical mesopore shape.

Figure 3(b) shows that the pore size distribution of BMS is at 3.28 and 9.22 nm respectively, corresponding with the two-distinct capillary condensation at  $P/P_0$  of 0.30 - 0.70 and  $P > 0.70$  in Fig. 3(a), which indicated the existence of two different size mesopore within the materials. While UMS-P123 and UMS-CTAB pore size distributions are of 4.20 and 3.28 nm respectively (Fig. 3(b)), which correspond to one capillary condensation at  $P/P_0$  of 0.30 - 0.70. From all the above results, it can be concluded that the large mesopores of BMS material in the range of 9 - 10 nm, while small mesopore in the range of 3 - 4 nm. As UMS-P123 and UMS-CTAB materials have pore in range of 3 - 4 nm [2, 6]. Therefore, the large mesopore of BMS were obtained from the material like SBA-15 which are the characteristic of Pluronic P123 [6, 13], and incorporated of CTAB [6]. In addition, the small mesopore of BMS were original from the parent templates. Theoretically, SBA-15 is a well-known mesoporous silica that prepare from the EO segments of the PEO-PPO-PEO template can insert into the silica wall as hybrid inorganic-organic composite framework [3]. When calcine to remove the template, some micropore and small mesopore are existed, connecting the main pore channels [6, 8]. So, BMS has the porosity than UMS-P123 and UMS-CTAB materials that are parent template [6, 10].

Physical properties including specific surface area, total volume and pore diameter are shown in Table 2. It is obvious that the specific surface area of BMS ( $> 670 \text{ m}^2/\text{g}$ ) is significantly higher than that of UMS-P123 as material like SBA-15 ( $337 \text{ m}^2/\text{g}$ ) and RHS ( $150 \text{ m}^2/\text{g}$ ) respectively, except UMS-CTAB material that has the highest surface area ( $1,118 \text{ m}^2/\text{g}$ ). Due to their long alkane chain of CTAB as the hydrophobic group to larger surface area and pore size [6, 9, 10]. Subsequently, as a result of the total pore volume was found to have decreased steadily; RHS ( $1.50 \text{ cm}^3/\text{g}$ ), BMS ( $1.30 \text{ cm}^3/\text{g}$ ), UMS-CTAB ( $1.00 \text{ cm}^3/\text{g}$ ) and UMS-P123 ( $0.29 \text{ cm}^3/\text{g}$ ), respectively. And corresponding to the decreased pore diameter of RHS (50 nm), BMS (9.22 & 3.28 nm), UMS-P123 (4.20 nm) and UMS-CTAB (3.28 nm), respectively. These results indicated that the synthesized material entered the large pores of RHS, deposited on the inner walls and the external surface of RHS, and formed small pores during the preparation of BMS [12]. It should be noted that the formation of as BMS was occurred from the swelling of Pluronic P123 micelles by the incorporation of CTAB micelles [29], as explain in Fig. 3.

### 3.5. Morphology

The morphologies, surface texture and porosity of BMS, UMS-P123, UMS-CTAB and RHS materials are revealed by the SEM and TEM images, as shown in Fig. 4. Figure 4(a, b, f, g) shows that bimodal mesoporous silica exhibited a hexagonal arrangement in terms of mesopores comprised of SBA-15 (aggregate cylindrical particles) and irregular particles. SBA-15 entering the pores of rice husk silica could be related to the large mesopores; specifically, on the walls of the pores and on the external surface, these were found to be interconnected. Similarly, the formation of mesopore templates during bimodal mesoporous silica preparation could explain the small mesopores (Pluronic P123 micelles by the incorporation of CTAB micelles) [6, 27]. The distribution of different pore sizes and  $\text{N}_2$  sorption isotherm are results which could be related to this. Figure 4(c, h) shows that UMS-P123 highlights a wide-scale collection of both sphere-shape and cylindrical particles which were in relation to silica particles formed with the template structure by Pluronic P123 [12]. Correspondingly, UMS-CTAB as shown in Fig. 4(d, i) cylindrical mesostructured and an arrangement with no order was shown by the materials, similar to the parent template [9, 10]. Figure 4(e) shows that rice husk silica material has better porosity and a rougher surface; within each particles, pores of different sizes can be seen as a result of the synthetic process occurring at the surface of material changes.

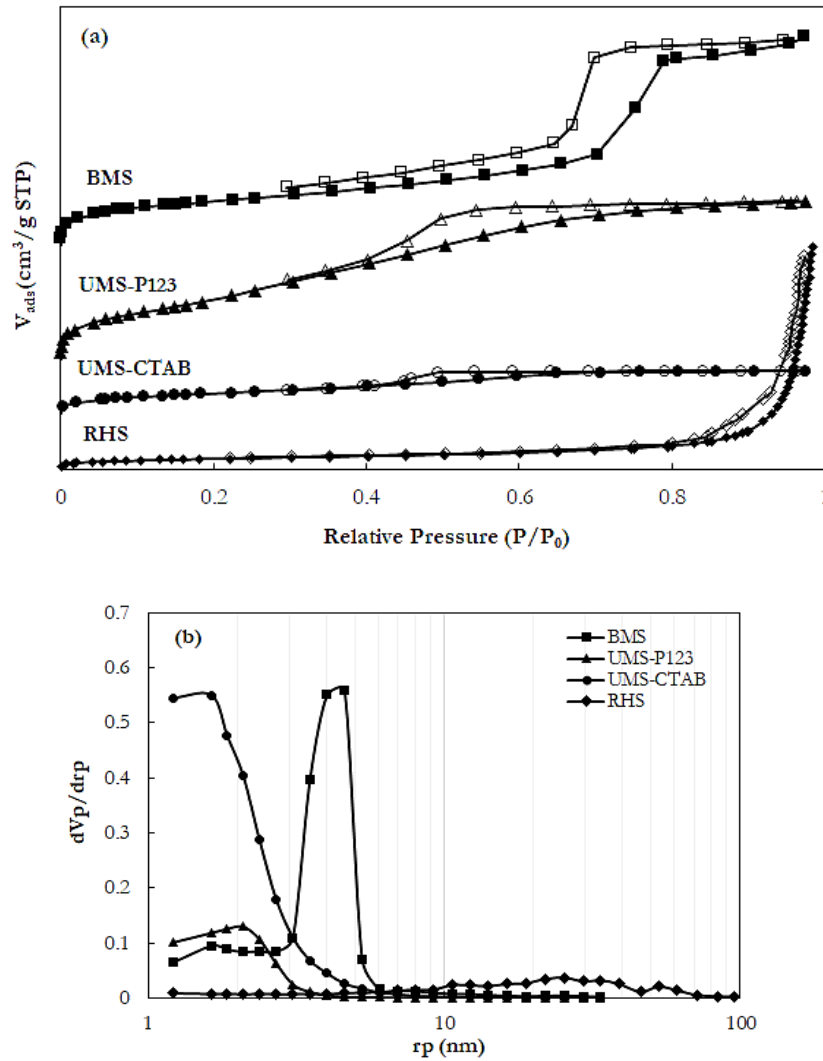
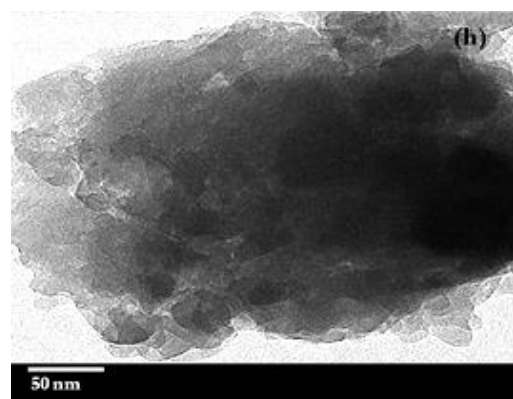
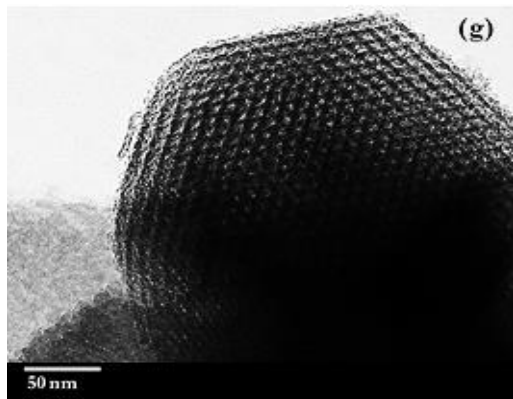
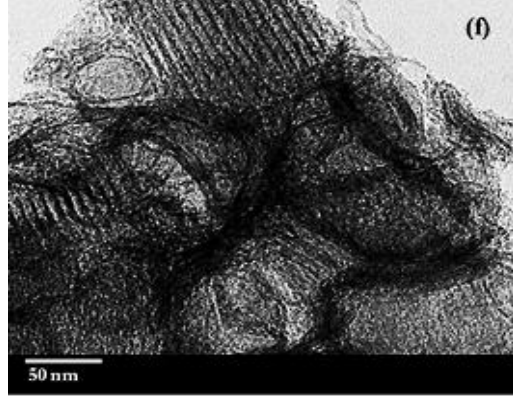
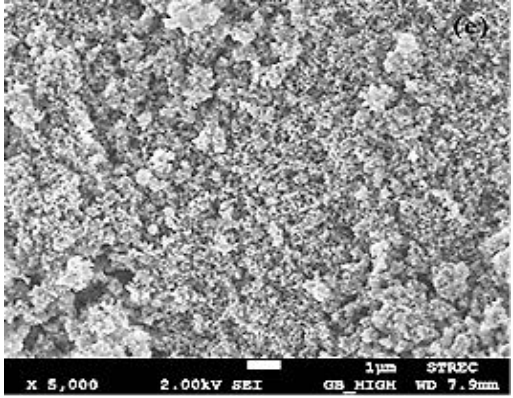
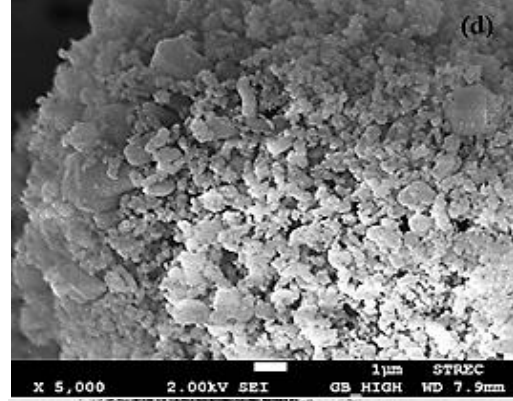
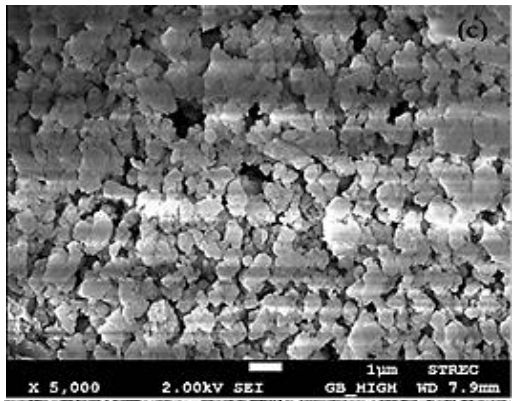
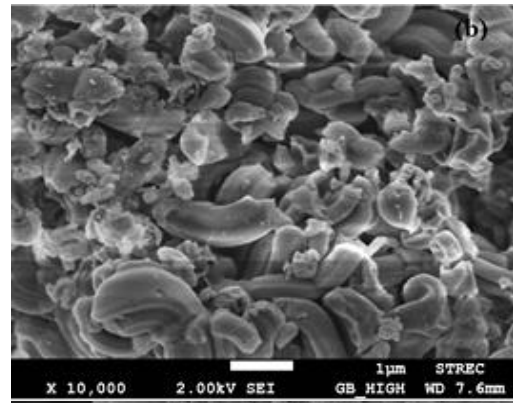
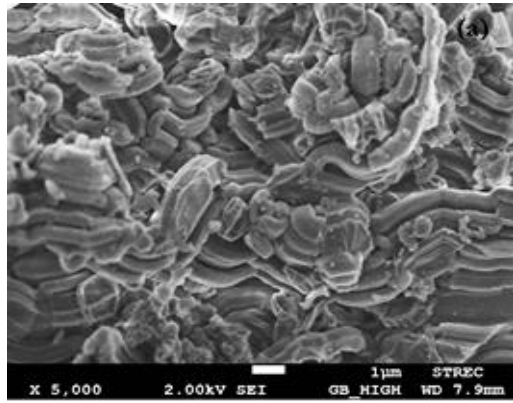


Fig. 3. (a) N<sub>2</sub> adsorption-desorption isotherms and (b) pore size distribution of BMS, UMS-P123, UMS-CTAB and RHS materials.

Table 2. Textural properties of all samples.

| Sample   | Textural properties                          |                                     |                               |
|----------|--|-------------------------------------|-------------------------------|
|          | Specific surface area<br>(m <sup>2</sup> /g) | Pore volume<br>(cm <sup>3</sup> /g) | Pore diameter average<br>(nm) |
| RHS      | 149  | 1.50                                | 51.0                          |
| BMS      | 672  | 1.30                                | 9.22 and 3.28                 |
| UMS-P123 | 336  | 0.29                                | 4.20                          |
| UMS-CTAB | 1118   | 1.00                                | 3.28                          |



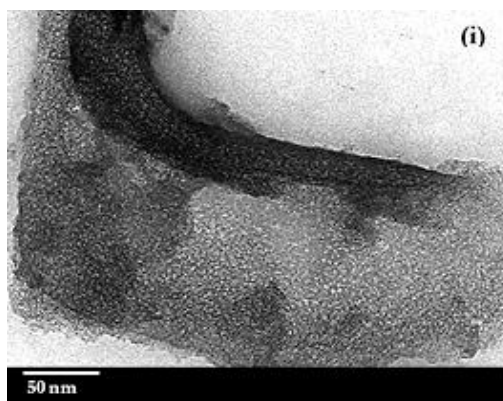


Fig. 4. SEM images of (a,b) BMS, (c) UMS-P123, (d) UMS-CTAB, (e) RHS; TEM images of (f,g) BMS, (h) UMS-P123 and (i) UMS-CTAB materials.

#### 4. Conclusion

Rice husk ash is an excellent raw material for the synthesis of bimodal mesoporous silica materials. The synthesis process was carried out by using silica derived from rice husk ash and the pore size and surface, can be controlled by using Pluronic P123 and CTAB with the aid of the sol-gel process. The mesostructure and physical properties of bimodal mesoporous silica materials were determined by X-ray diffraction, X-ray fluorescence spectrometer, Fourier-transform infrared spectrometer, N<sub>2</sub> adsorption-desorption isotherm, SEM and TEM techniques especially, BMS has a distinctive of two mesopore and large surface area. Therefore, the use of rice husk ash as raw material instead of commercial silica gave the similar properties of BMS material as well as giving the environmental benefits and the renewable resources.

#### Acknowledgements

The authors would like to thank the National Research Council of Thailand and Grant of Chulalongkorn University 'Ratchadaphiseksomphot Endowment Fund' for financial support of this research. Also we thank Interdisciplinary Program of Environmental Science, Graduate School, Chulalongkorn University for facility support.

#### References

- [1] L. Yang, H. Wu, J. Jia, B. Ma, and J. Li, "Synthesis of bimodal mesoporous silica with coexisting phases by co-hydrothermal aging route with P123 containing gel and F127 containing gel," *Microporous and Mesoporous Materials*, vol. 253, pp. 151-159, 2017.
- [2] O. A. Anunziata, A. R. Beltramone, M. L. Martínez, and L. L. Belon, "Synthesis and characterization of SBA-3, SBA-15, and SBA-1 nanostructured catalytic materials," *Journal of Colloid and Interface Science*, vol. 315, no. 1, pp. 184-190, 2007.
- [3] L. Gao, J. Sun, and Y. Li, "Functionalized bimodal mesoporous silicas as carriers for controlled aspirin delivery," *Journal of Solid State Chemistry*, vol. 184, no. 8, pp. 1909-1914, 2011.
- [4] S. M. L. dos Santos, K. A. B. Nogueira, M. de Souza Gama, J. D. F. Lima, I. J. da Silva Júnior, and D. C. S. de Azevedo, "Synthesis and characterization of ordered mesoporous silica (SBA-15 and SBA-16) for adsorption of biomolecules," *Microporous and Mesoporous Materials*, vol. 180, pp. 284-292, 2013.
- [5] S. Rani, K. Sumanjit, and R. Mahajan, "Synthesis of mesoporous material SBA-3 for adsorption of dye congo red," *Desalination and Water Treatment*, pp. 1-12, 2014.
- [6] D. Zhao, Y. Wan, and W. Zhou, *Ordered Mesoporous Materials*. Weinheim, Germany: Wiley-VCH, 2013.
- [7] M. J. Reber and D. Bruhwiler, "Bimodal mesoporous silica with bottleneck pores," *Dalton Transactions*, vol. 44, no. 41, pp. 17960-17967, 2015.
- [8] F. Zhang, Y. Yan, Y. Meng, Y. Xia, B. Tu, and D. Zhao, "Ordered bimodal mesoporous silica with tunable pore structure and morphology," *Microporous and Mesoporous Materials*, vol. 98, no. 1, pp. 6-15, 2007.

- [9] T. Witoon, M. Chareonpanich, and J. Limtrakul, "Synthesis of bimodal porous silica from rice husk ash via sol-gel process using chitosan as template," *Materials Letters*, vol. 62, no. 10, pp. 1476-1479, 2008.
- [10] O. Jullaphan, T. Witoon, and M. Chareonpanich, "Synthesis of mixed-phase uniformly infiltrated SBA-3-like in SBA-15 bimodal mesoporous silica from rice husk ash," *Materials Letters*, vol. 63, no. 15, pp. 1303-1306, 2009.
- [11] X. Zhang, C. Guo, X. Wang, and Y. Wu, "Synthesis and characterization of bimodal mesoporous silica," *Journal of Wuban University of Technology-Mater. Sci. Ed.*, vol. 27, no. 6, pp. 1084-1088, 2012.
- [12] S. M. L. dos Santos, K. A. B. Nogueira, M. de Souza Gama, J. D. F. Lima, I. J. da Silva Júnior, and D. C. S. de Azevedo, "Synthesis and characterization of ordered mesoporous silica (SBA-15 and SBA-16) for adsorption of biomolecules," *Microporous and Mesoporous Materials*, vol. 180, no. Supplement C, pp. 284-292, 2013.
- [13] D. Zhao, J. Sun, Q. Li, and G. D. Stucky, "Morphological control of highly ordered mesoporous silica SBA-15," *Chemistry of Materials*, vol. 12, no. 2, pp. 275-279, 2000.
- [14] W. Clowutimon, P. Kitchaiya, and P. Assawasaengrat, "Adsorption of free fatty acid from crude palm oil on magnesium silicate derived from rice husk," *Engineering Journal*, vol. 15, no. 3, pp. 15-26, 2011.
- [15] N. Saengprachum and S. Pengprecha, "Preparation and characterization of aluminum oxide coated extracted silica from rice husk ash for monoglyceride removal in crude biodiesel production," *Journal of the Taiwan Institute of Chemical Engineers*, vol. 58, pp. 441-450, 2016.
- [16] M. C. Manique, C. S. Faccini, B. Onorevoli, E. V. Benvenuti, and E. B. Caramão, "Rice husk ash as an adsorbent for purifying biodiesel from waste frying oil," *Fuel*, vol. 92, no. 1, pp. 56-61, 2012.
- [17] V. P. Della, I. Kühn, and D. Hotza, "Rice husk ash as an alternate source for active silica production," *Materials Letters*, vol. 57, no. 4, pp. 818-821, 2002.
- [18] U. Kalapathy, A. Proctor, and J. Shultz, "A simple method for production of pure silica from rice hull ash," *Bioresource Technology*, vol. 73, no. 3, pp. 257-262, 2000.
- [19] U. R. Lakshmi, V. C. Srivastava, I. D. Mall, and D. H. Lataye, "Rice husk ash as an effective adsorbent: Evaluation of adsorptive characteristics for Indigo Carmine dye," *Journal of Environmental Management*, vol. 90, no. 2, pp. 710-720, 2009.
- [20] J. Pothongkom, "Glycerin removal in biodiesel purification process by adsorbent from rice husk," Master's degree, Graduate school, Chulalongkorn University, 2011.
- [21] U. Kalapathy, A. Proctor, and J. Shultz, "An improved method for production of silica from rice hull ash," *Bioresource Technology*, vol. 85, no. 3, pp. 285-289, 2002.
- [22] R. S. McDonald, "Surface functionality of amorphous silica by infrared spectroscopy," *The Journal of Physical Chemistry*, vol. 62, no. 10, pp. 1168-1178, 1958.
- [23] F. Ahangaran, A. Hassanzadeh, and S. Nouri, "Surface modification of Fe<sub>3</sub>O<sub>4</sub>@SiO<sub>2</sub> microsphere by silane coupling agent," *International Nano Letters*, vol. 3, no. 1, p. 23, 2013.
- [24] R. Nariyal, P. Kothari, and B. Bisht, "FTIR measurements of SiO<sub>2</sub> glass prepared by sol-gel technique," *Chemical Science Transactions*, vol. 3, no. 3, pp. 1064-1066, 2014.
- [25] N. Pijarn, A. Jaroenworuluck, W. Sunsaneeyametha, and R. Stevens, "Synthesis and characterization of nanosized-silica gels formed under controlled conditions," *Powder Technology*, vol. 203, no. 3, pp. 462-468, 2010.
- [26] T. Witoon and M. Chareonpanich, "Effect of pore size and surface chemistry of porous silica on CO<sub>2</sub> adsorption," *Songklanakarin Journal of Science & Technology*, vol. 34, no. 4, 2012.
- [27] Z. A. AlOthman, "A review: fundamental aspects of silicate mesoporous materials," *Materials*, vol. 5, no. 12, pp. 2874-2902, 2012.
- [28] B. G. Trewyn, I. I. Slowing, S. Giri, H.-T. Chen, and V. S.-Y. Lin, "Synthesis and functionalization of a mesoporous silica nanoparticle based on the sol-gel process and applications in controlled release," *Accounts of Chemical Research*, vol. 40, no. 9, pp. 846-853, 2007.
- [29] S. Rani, K. Sumanjit, and R. K. Mahajan, "Synthesis of mesoporous material SBA-3 for adsorption of dye congo red," *Desalination and Water Treatment*, vol. 57, no. 8, pp. 3720-3731, 2016.